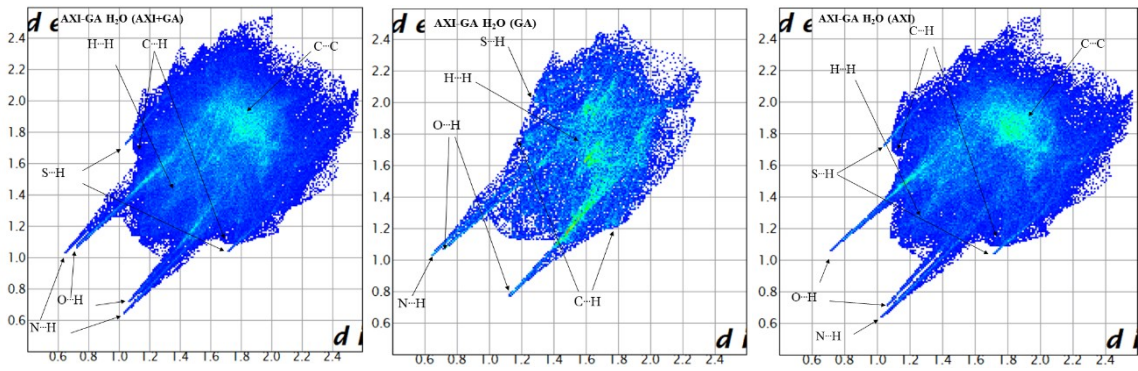


## Supplementary data for

### **Two anhydrous forms and one monohydrate of a cocrystal of axitinib and glutaric acid: characterization, property evaluation and phase transition study**

**Bo-Ying Ren<sup>a</sup>, Xia-Lin Dai<sup>b</sup>, Jia-Mei Chen<sup>\*b</sup>, Tong-Bu Lu<sup>a</sup>**

(a)



(b)

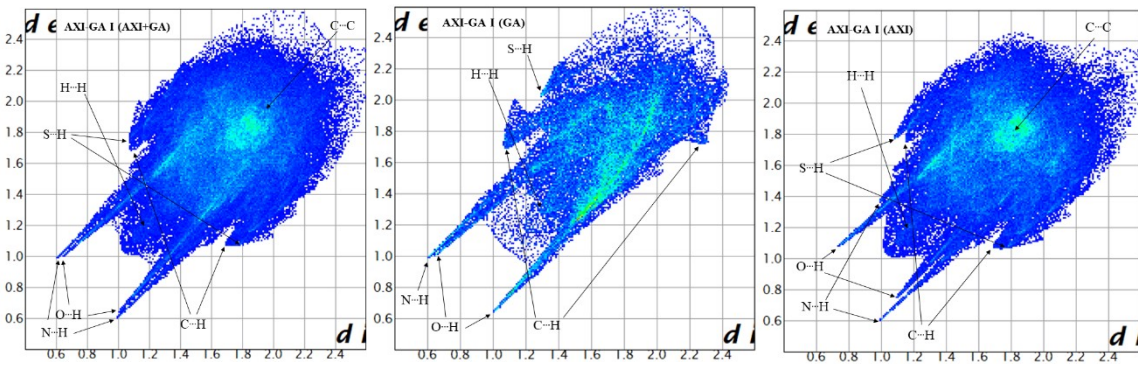


**Figure S1.** 2D fingerprint plots of the Hirshfeld surfaces of (a) AXI-GA·H<sub>2</sub>O (b) AXI-GA I.

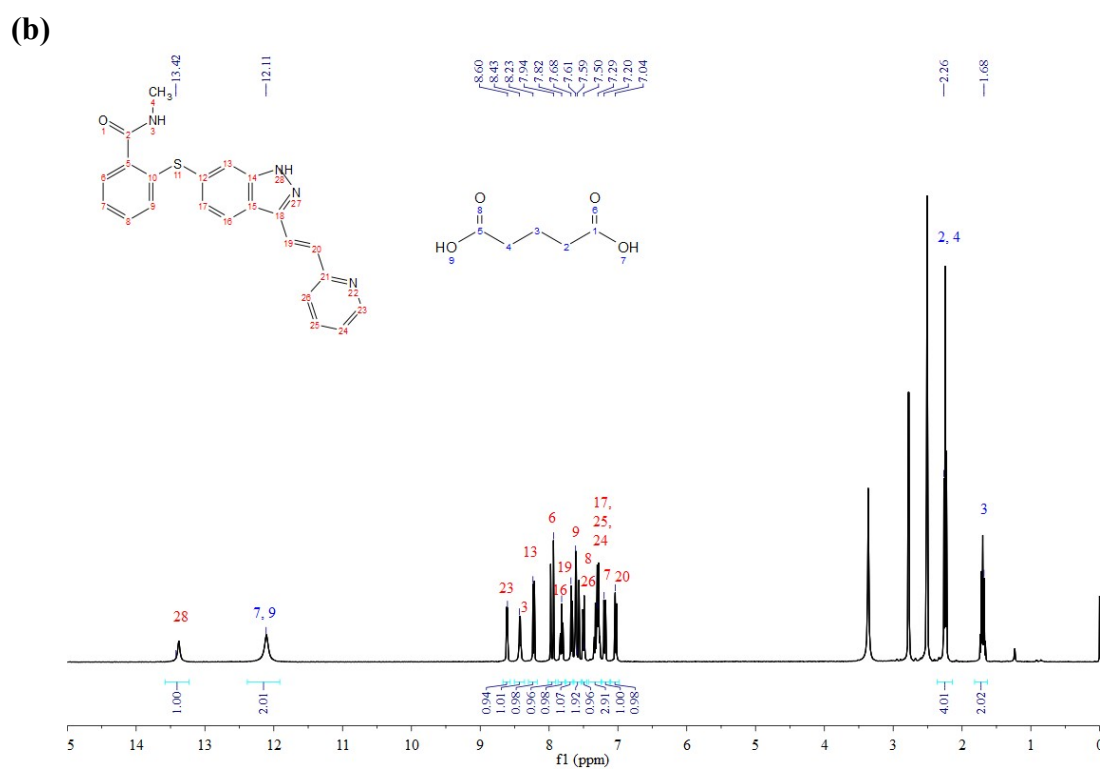
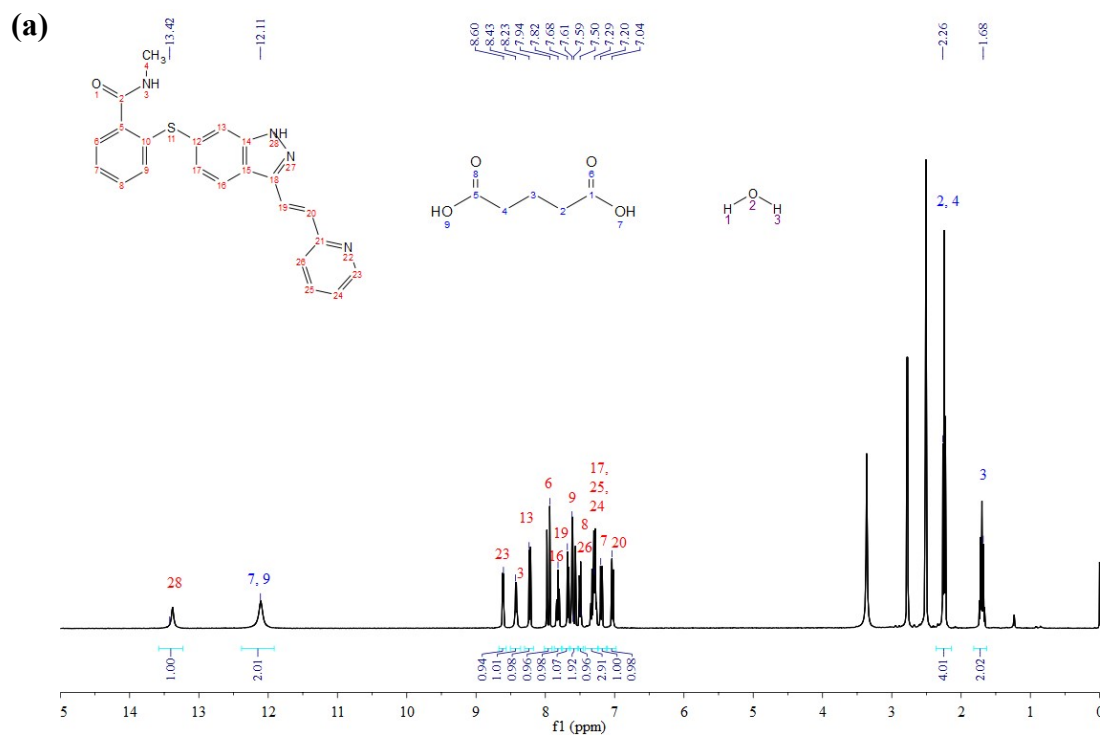


**Figure S2.**  $^1\text{H}$  NMR spectra of (a) **AXI-GA·H<sub>2</sub>O** and (b) **AXI-GA I**.

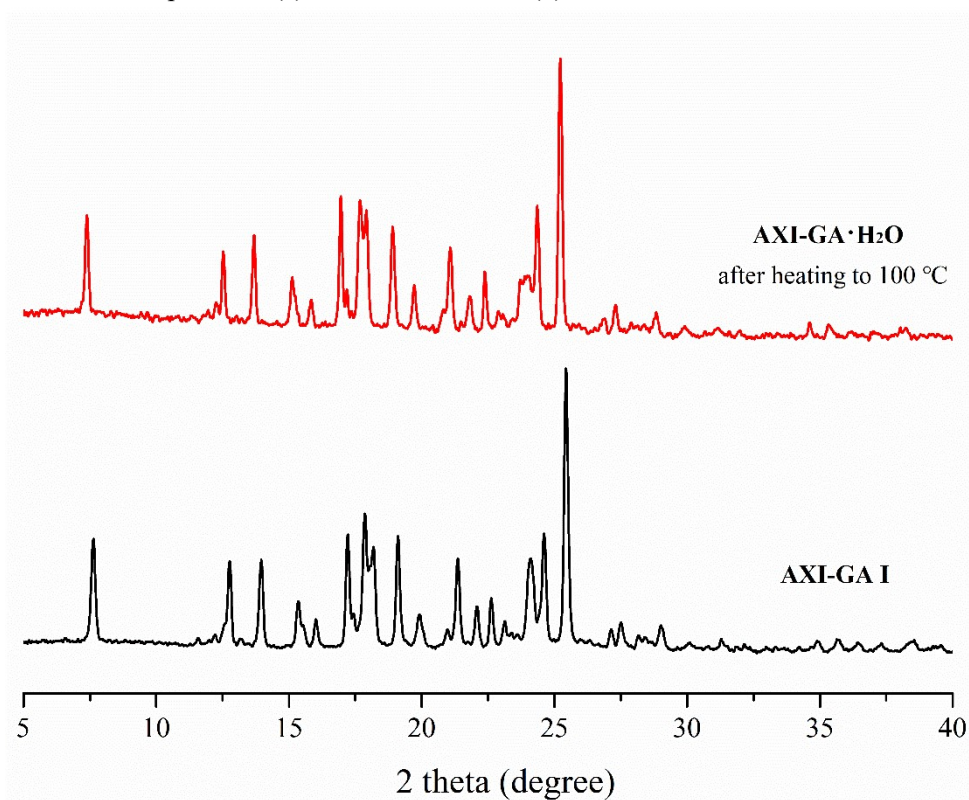


**Figure S3.** PXRD patterns of **AXI-GA·H<sub>2</sub>O** after heating to 100 °C.

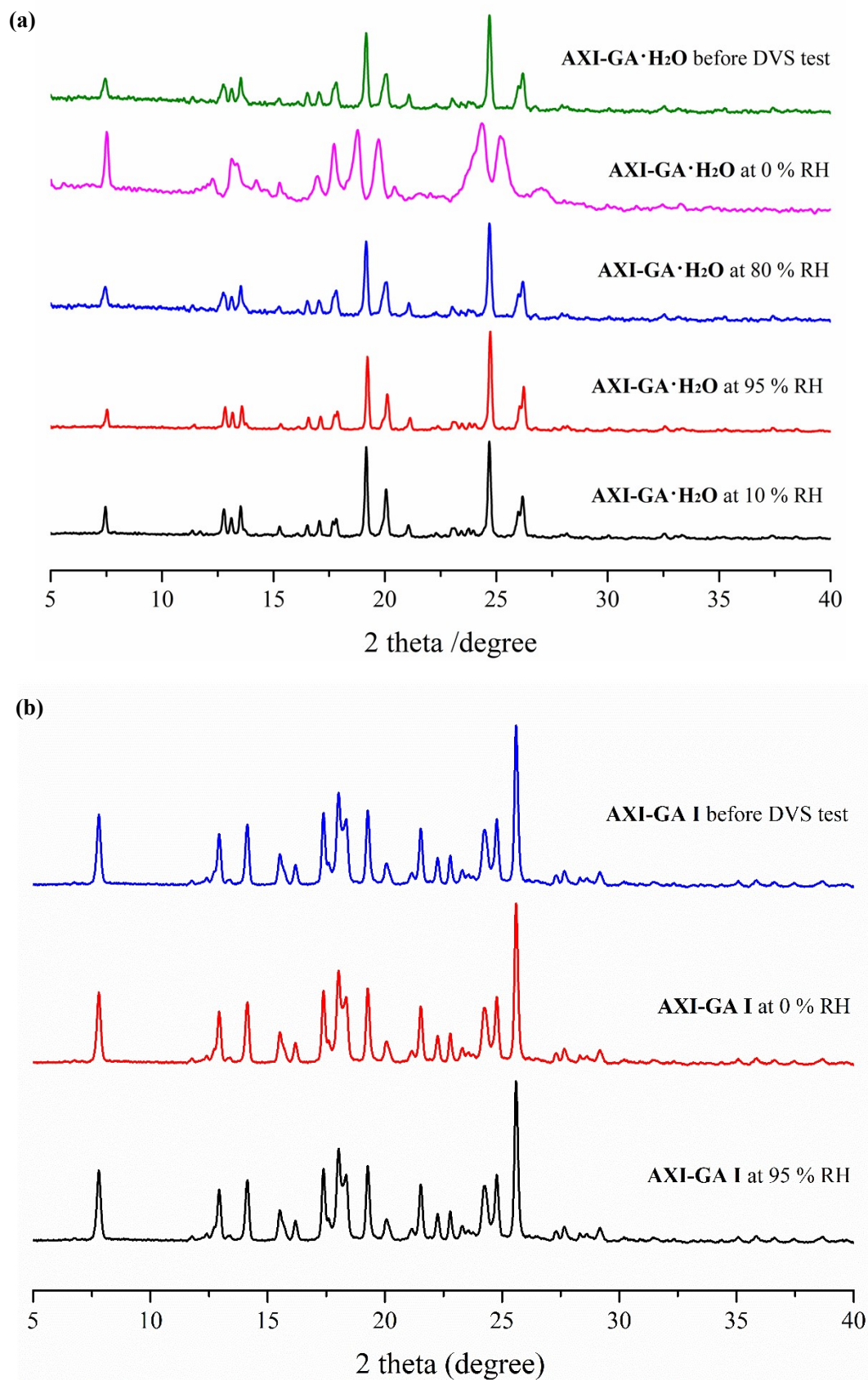
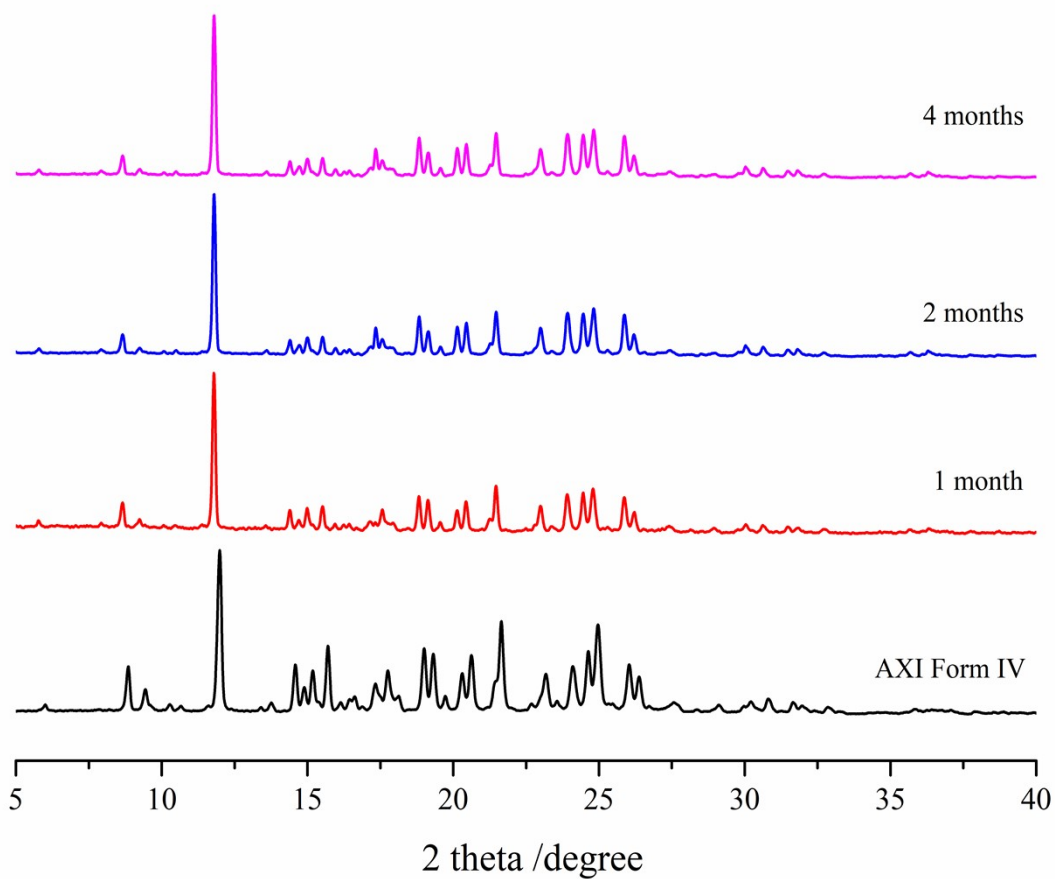
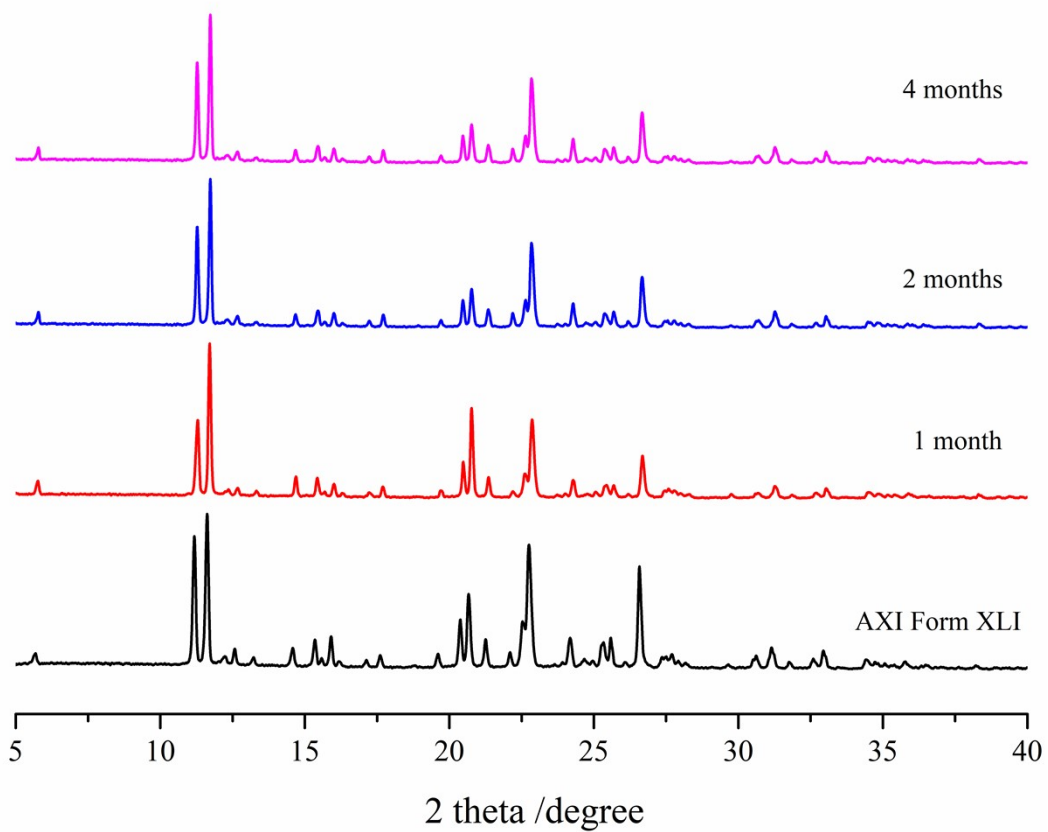


**Figure S4.** PXRD patterns of (a) AXI-GA·H<sub>2</sub>O and (b) AXI-GA I involving in DVS test. A phase change from AXI-GA·H<sub>2</sub>O to a metastable form (referring to AXI-GA II) was observed at 0% RH, which converted back to AXI-GA·H<sub>2</sub>O at 80% RH.

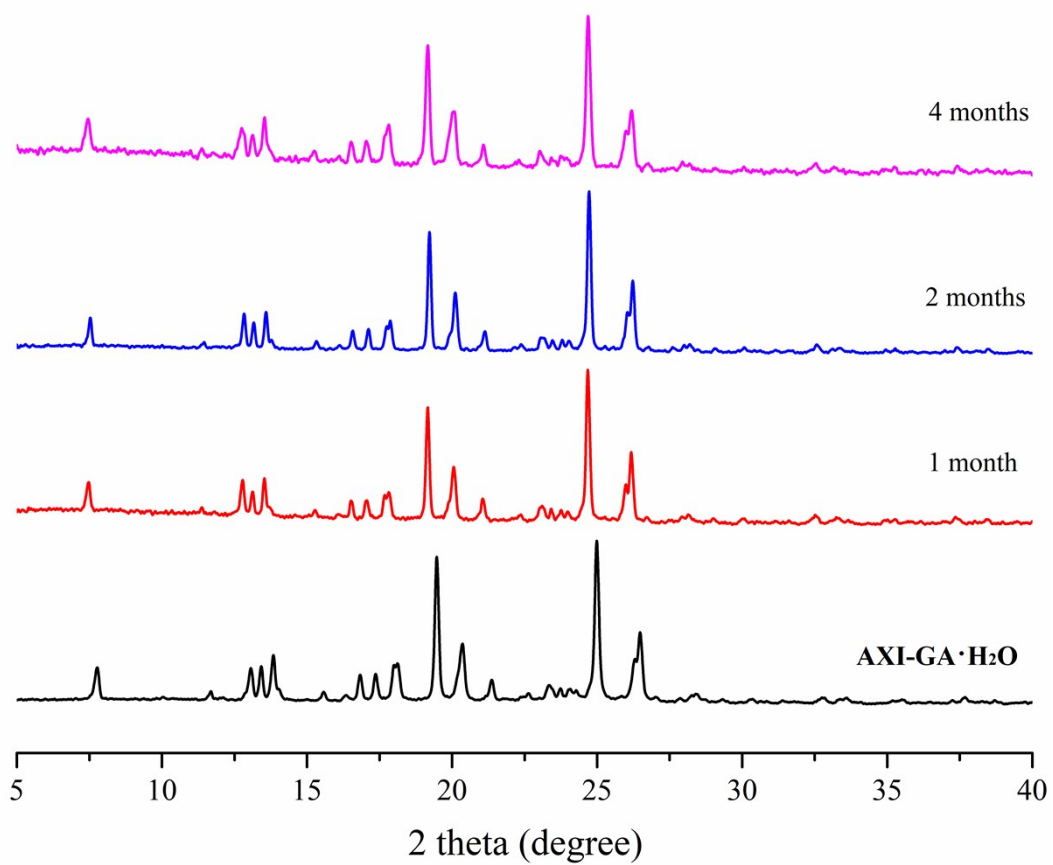
(a)



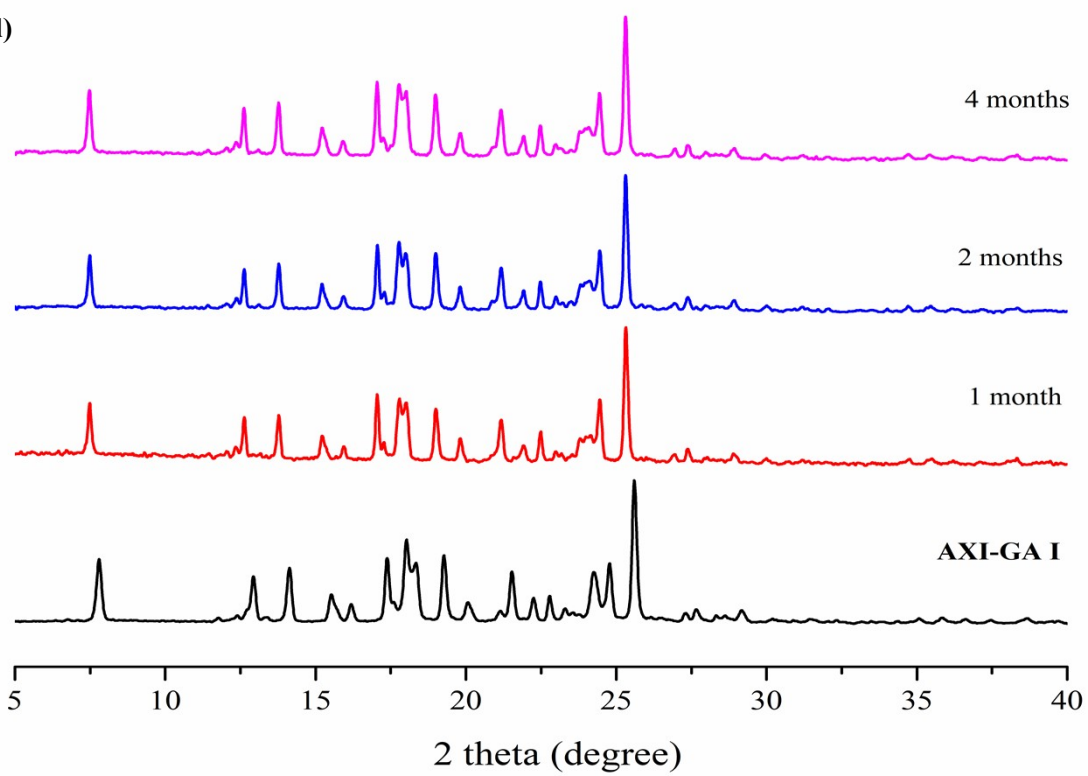
(b)



(c)



(d)



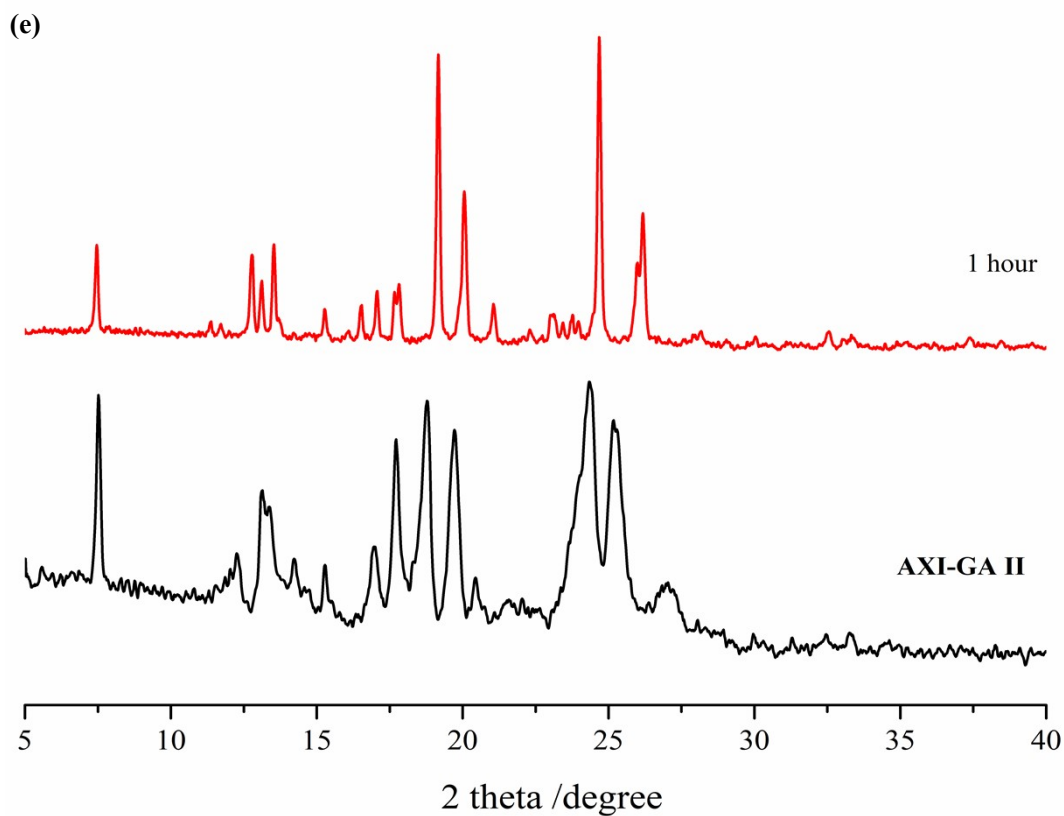


**Figure S5.** PXRD patterns of (a) AXI Form IV, (b) AXI Form XLI, (c) AXI-GA·H<sub>2</sub>O, (d) AXI-GA I and (e) AXI-GA II under 40 °C/75% RH accelerated conditions.

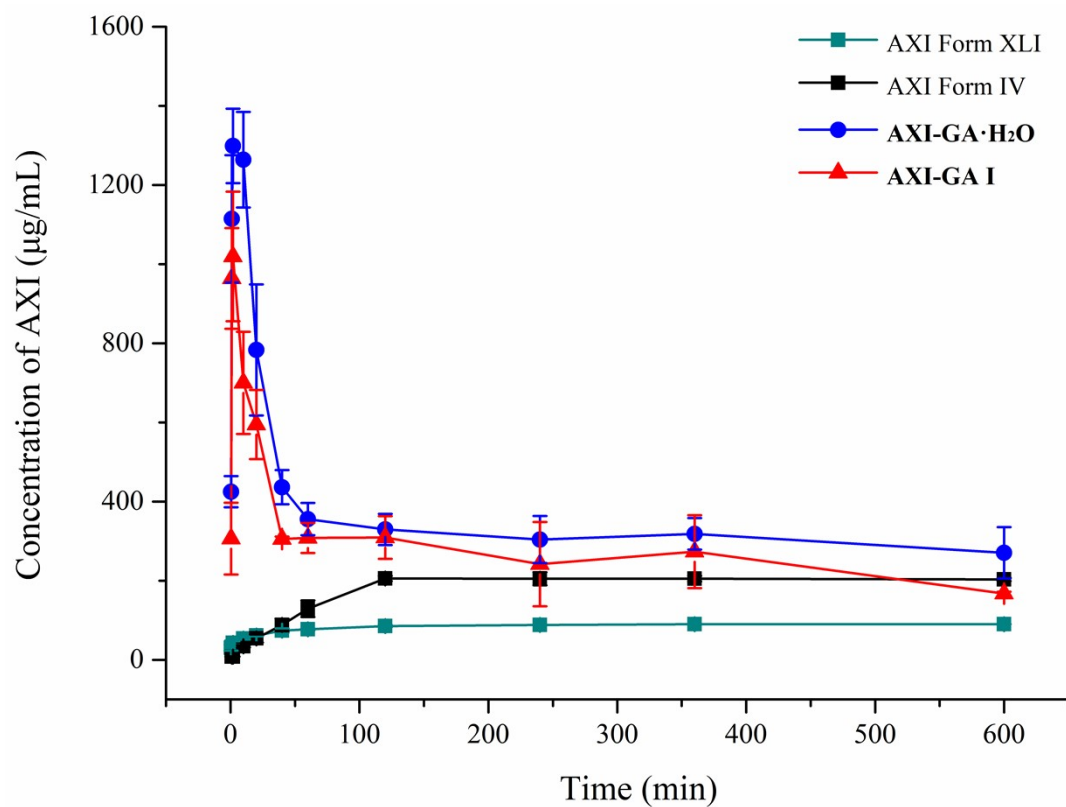


**Figure S6.** Powder dissolution profiles for AXI-GA·H<sub>2</sub>O, AXI-GA I and AXI within 10 h.



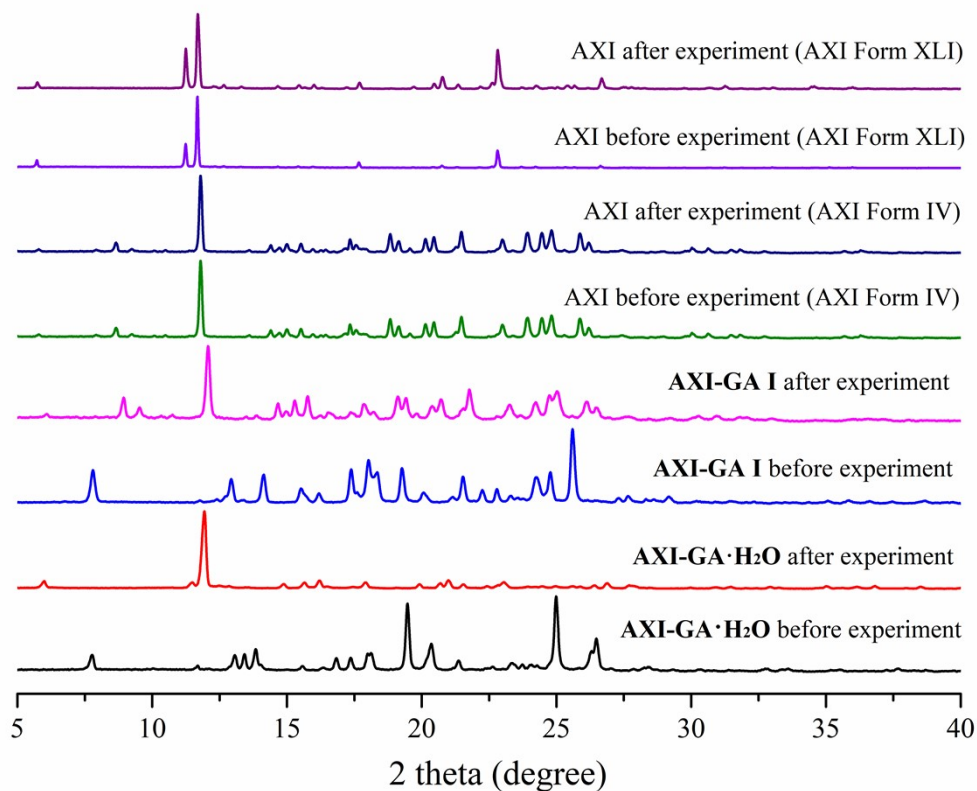


**Figure S7.** PXRD patterns of the residual solids of AXI-GA·H<sub>2</sub>O, AXI-GA I, AXI Form IV and XLI after powder dissolution experiments.

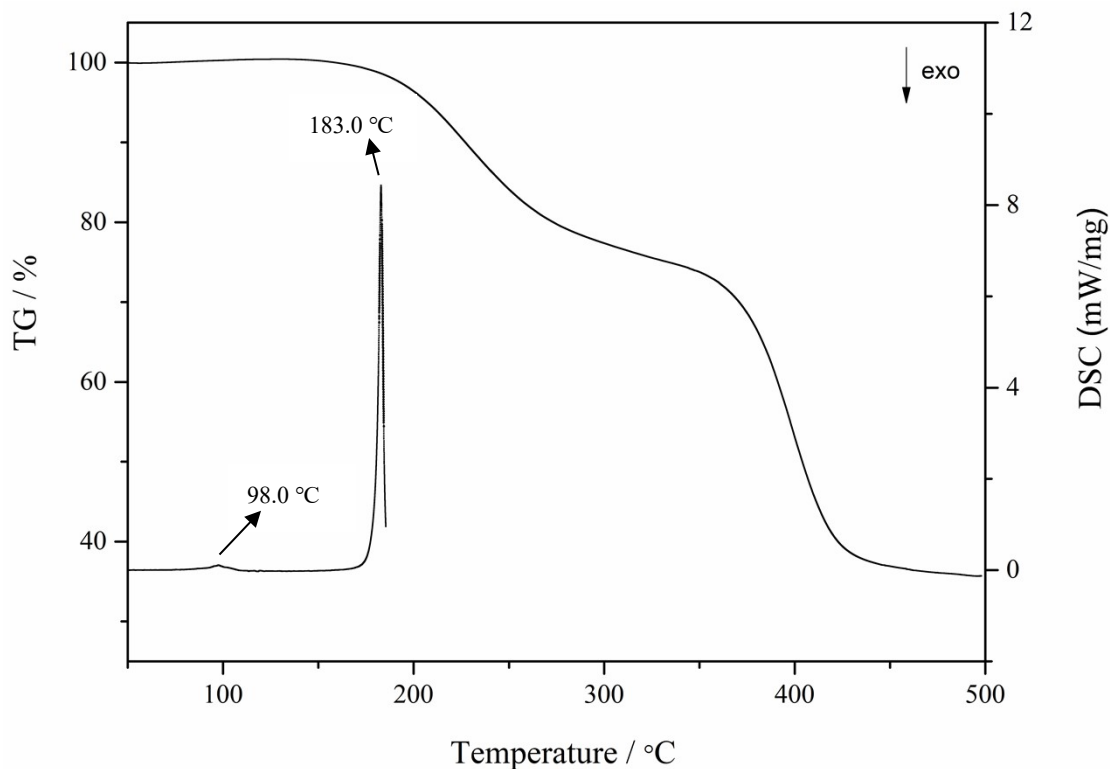


**Figure S8.** TG-DSC curves of AXI-GA II.

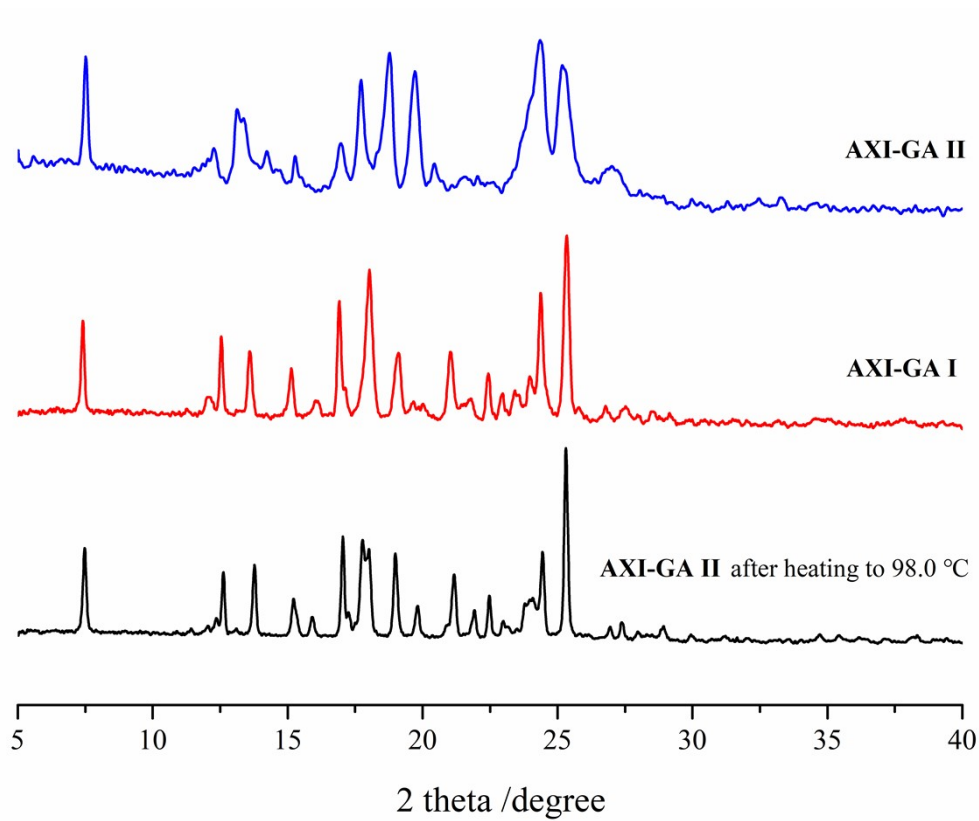


**Figure S9.** PXRD patterns of AXI-GA II and its powder sample heating after 98.0 °C.

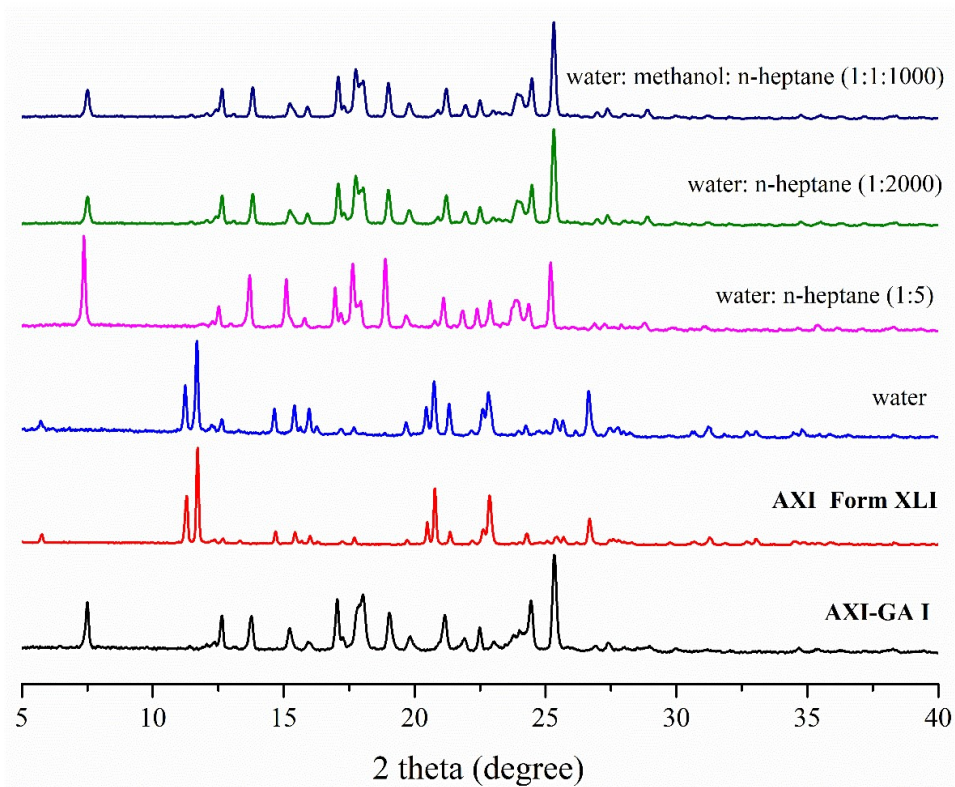


**Figure S10.** PXRD patterns of the residual solids of powdered 1:1 mixture of AXI-GA·H<sub>2</sub>O and AXI-GA I after slurry in various solvents.